



# Fracture Analysis of a Case-Hardened Kingpin

Tuğrul Soyusinmez<sup>1\*</sup> , Oğuzcan Güzelipek<sup>1</sup> , Tolga Palandüz<sup>1</sup> , Onur Ertuğrul<sup>2</sup> 

<sup>1</sup>Totomak A.Ş., İzmir, Turkey

<sup>2</sup>İzmir Katip Çelebi University, Dept. of Materials Science and Engineering, İzmir, Turkey

## Abstract

Kingpin parts are one of the critical products for heavy vehicles and are generally made of 20MnCr5 steel. A kingpin is a heavy metal cylindrical pin that is located underneath the front end of the trailer. The kingpin is the mechanism on the trailer that locks it to a road tractor. The parts in this study have undergone to case hardening heat treatment after the rough machining operation. During the operation in the assembly line, cracks have been realized on the surface of the parts. In this study, the kingpin parts are examined with optical microscopy, Scanning Electron Microscopy (SEM), hardness tests and %C potential analysis in order to determine the potential causes of the crack formations. By the help of the analysis, the presence of cracks became clear. There are no signs of hydrogen embrittlement. The exact outcome of the fracture could not be determined. It is seen that heat treatment of the parts is not homogeneously obtained throughout their surfaces or desired volume, and therefore fractures occur. With the present structure, it can be expected that even a low dynamic load can lead to breakage. As a result, the investigations suggest that the parts were exposed to inappropriate heat treatment parameters.

**Keywords:** Kingpin, Case Hardening, Scanning Electron Microscopy (SEM), Crack formation, 20MnCr5 steel

## 1. INTRODUCTION

The n-trailer system is a unlike a flat system, who is flat (or linearizing) outputs are the Cartesian coordinates of the middle point of last trailer's rear axle. Mobile robots with trailers are flat systems as soon as the trailers are hitched to the middle point of the axle of the previous ones. Placing the king pin off the axle will cause the system not to be straight. The placement of the kingpin outside the axle makes the system not flat.[1] The kingpin sliding mechanism allows the kingpin to slide along the axle of the previous trailer. From the perspective of routing and control theory, a natural question is whether the system remains flat. It is also proved that the n-trailer system equipped with a sliding kingpin mechanism is a differentially flat system [2].

Steels used for surface hardening generally contain a carbon content of about 0.2%, and the carbon content of the carburized layer generally being controlled at between 0.7 and 1% C. However, the carbon content on the surface should generally not exceed 0.9% because high carbon content can result in retained austenite and brittle martensite (due to the formation of proeutectoid carbides on the grain boundaries) [3].

Surface hardening is a process that has been used for many years to improve the surface hardness of metals. Fast heating and rapid quenching methods are used to increase the surface hardness. Surface hardening is observed with the changes provided in the microstructure [4]. The compressive residual stresses prolong the fatigue lifetime of the hardened component. In the surface induction hardening process, heating is very fast and directly followed by quenching, so the generation of residual stresses is more complex than the common hardening process [5]. Calculating the variation of heat generation rate in components with a complex geometry is difficult, therefore the experimental measurements of surface heat fluxes are also used. Many finite element studies focused on the prediction of residual stresses in components during heating and quenching and a few papers on the surface induction hardening have been published in the past years. The finite element method (FEM) makes it possible to estimate the residual stresses in components during heating and quenching to determine the relationship between process parameters and the mechanical properties of the material being processed [6].

For iron or steel parts with low carbon content, which has poor hardenability due to the chemical composition, the

\* Corresponding author  
Email: tsoyusinmez@totomak.com.tr



case hardening process involves infusing additional carbon or nitrogen into the surface layer. Case hardening is usually applied after the part has been formed into its final shape, however, can also be applied to increase the hardening element content of bars to be used in a pattern welding or similar process: Case hardening process is applied intensively on parts subjected to high pressure or sharp impacts. Firing pins, rifle faces, engine crankshafts can be shown as examples of parts that have been processed. In these cases, the surface may be hardened selectively, leaving the center of the part in its original tough state [7,8].

Stress corrosion cracking and intergranular corrosion of are the most important corrosion types those affect the service behavior of austenitic stainless steels. Dissimilar material and environmental factors affect stress corrosion cracking behavior of austenitic stainless steels. The environmental factors include the processes of forming by cold plastic deformation and seam welding. The latter justifies that there is a growing interest in knowing the effect that prior to cold work and sensitization treatment have on the stress corrosion cracking behavior of these types of materials [9,10].

In this work, the reasons of a sudden failure of a steel part during its assembly have been investigated in detail. By conducting many experimental studies, a detailed fracture analysis has been made. The aim of the analysis is also to investigate the effects of the heat treatment parameters for determining the fracture of the kingpin parts.

**2. MATERIAL AND METHODS**

The spectral analysis, metallography and fractography studies, SEM analysis and hardness tests were carried out for the 16MnCr5 steel parts, respectively. The image of the kingpin part broken in assembly lines is shown in Figure 1. The chemical composition of the analyzed 16MnCr5 steel is shown in Table 1, and the mechanical properties are given in Table 2.

**Table 1.** Chemical composition of 16MnCr5 (1.7131) steel (wt.%)

C	Si	Mn	P	S	Cr
0.14 - 0.19	max 0.4	1 - 1.3	max 0.025	max 0.035	0.8 - 1.1



**Table 2.** Mechanical properties of the 16MnCr5 (1.7131) steel

Property	Value
Nominal thickness (mm):	to 16
Rm - Tensile strength (MPa) hardening and tempering at 200°C	1000
Rm - Tensile strength (MPa)	550
Rp0.2 0.2% proof strength (MPa)	420
A - Min. elongation Lo = 80 mm (%)	21
Z - Reduction in cross section on fracture (%)	62-64
Vickers hardness (HV)	170

Before the macroscopic examinations, the fracture surfaces were cleaned in an ultrasonic bath, and then examined under a stereo microscope. For further investigation, samples were prepared through the examined part. The locations where samples were taken out are shown in Figure 2. The samples were taken from three different positions and have been encoded as follows: RD-Radius (05-20-0619-1), FR-Fracture surface (05-20-0619-2), and FL-Flange (05-20-0619-3). Representative coding's are given in Table 3.

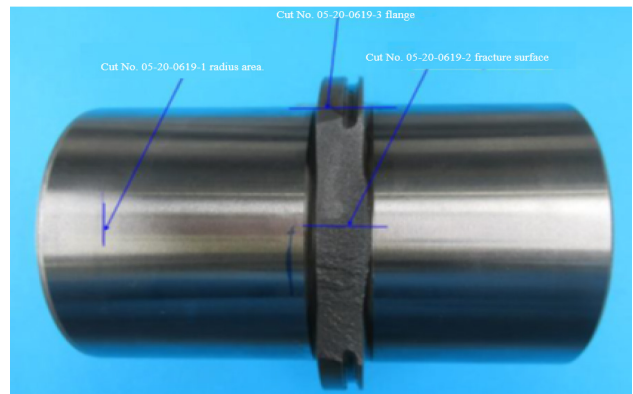


**Figure 2.** The locations where samples were taken out

**Table 3.** Representative coding's belong to three different locations.

Sample Code	Location	Long name
RD	Radius	05-20-0619-1
FR	Fracture surface	05-20-0619-2
FL	Flange	05-20-0619-3

In order to understand the reasons of the kingpin's failure, the broken failure areas were examined by Scanning Electron Microscopy (SEM). Also, Vickers set hardness tests, using 1 kg load, were carried out on from the surface of the

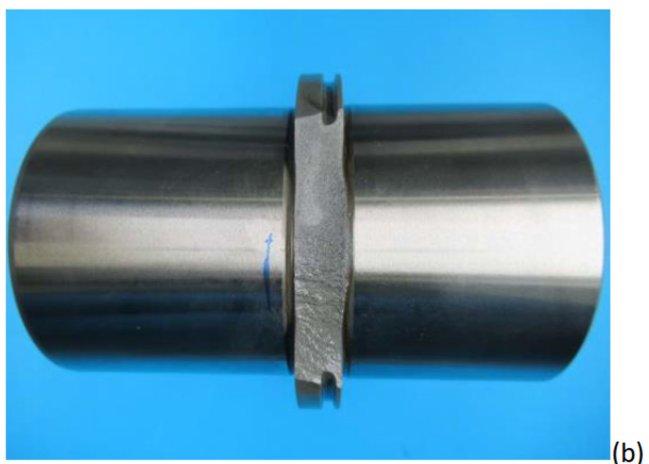


**Figure 1.** Images of the (a)original, and (b)broken kingpin part

samples after heat treatment in order to determine the hardness depth of the parts.

### 3. RESULTS AND DISCUSSION

All the samples were examined from their cross-section by a light microscope. The images of the RD sample from its surface area with different magnifications have been shown in Figure 3, which present mainly the martensitic microstructure. And the microstructure belongs to the center part of the radius section containing mixed structure of bainite and coarse martensite phases which is shown in Figure 4. Moreover, the images from the cross section of the fracture surface with different magnifications have been shown in Figure 5. It is clearly shown here that the microstructure

consists of a mixed structure containing bainite and coarse martensite phases.

The surface area belongs to flange section contain hard martensitic structure as shown in Figure 6. And the microstructure belongs to the center part of the flange section having the mixed structure of bainite and coarse martensite phases are shown in Figure 7.

The metallographic investigations for both RD and FL samples show that there is a hard martensitic structure without any mesh or bone type carbide at the surface zones. In the center, there is an inhomogeneous mixed structure of bainite and coarse martensite phases. It can be assumed that the structure shows high strength. Based on the cen-

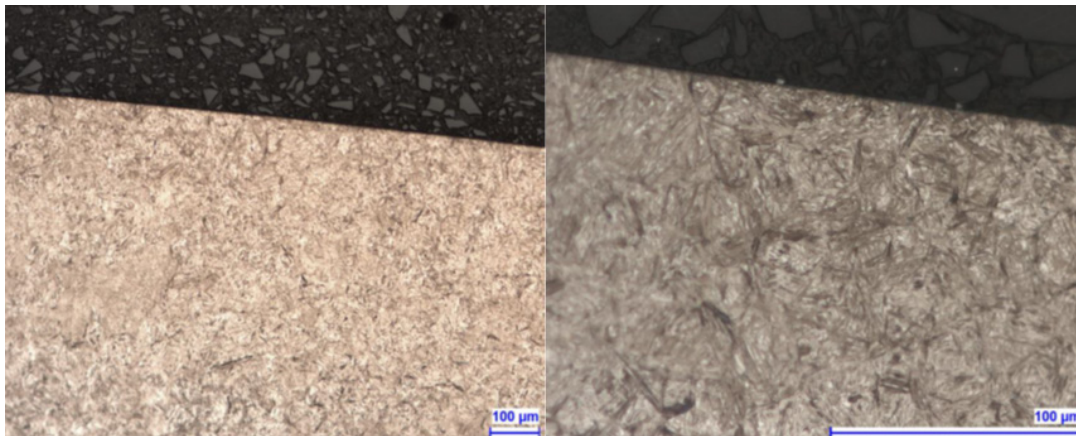


Figure 3. Surface structure of the RD sample showing the martensitic structure

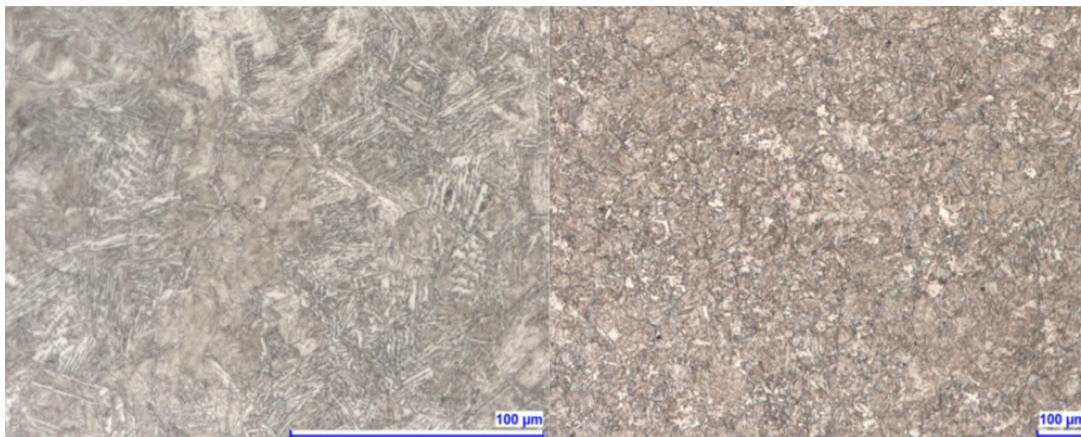


Figure 4. Mixed structure of bainite and coarse martensite phases on the center part of RD sample



Figure 5. Images of the FR sample showing a mixed structure of bainite and coarse martensite phases

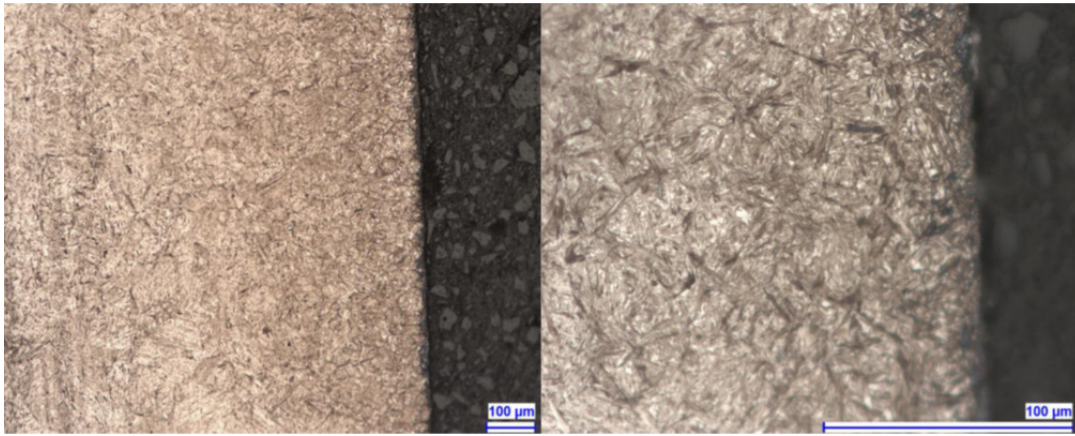


Figure 6. Surface structure of the FL sample having hard martensitic structure

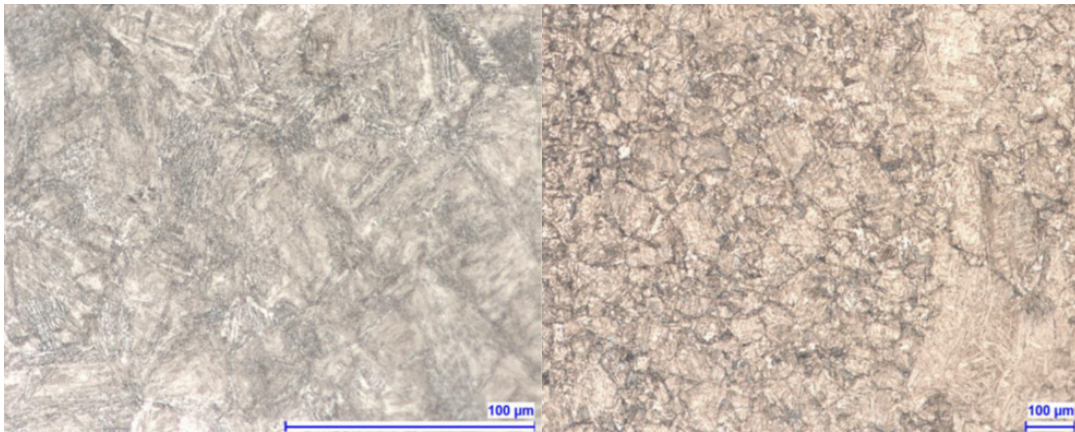


Figure 7. Flange area mixed structure of bainite and coarse martensite components

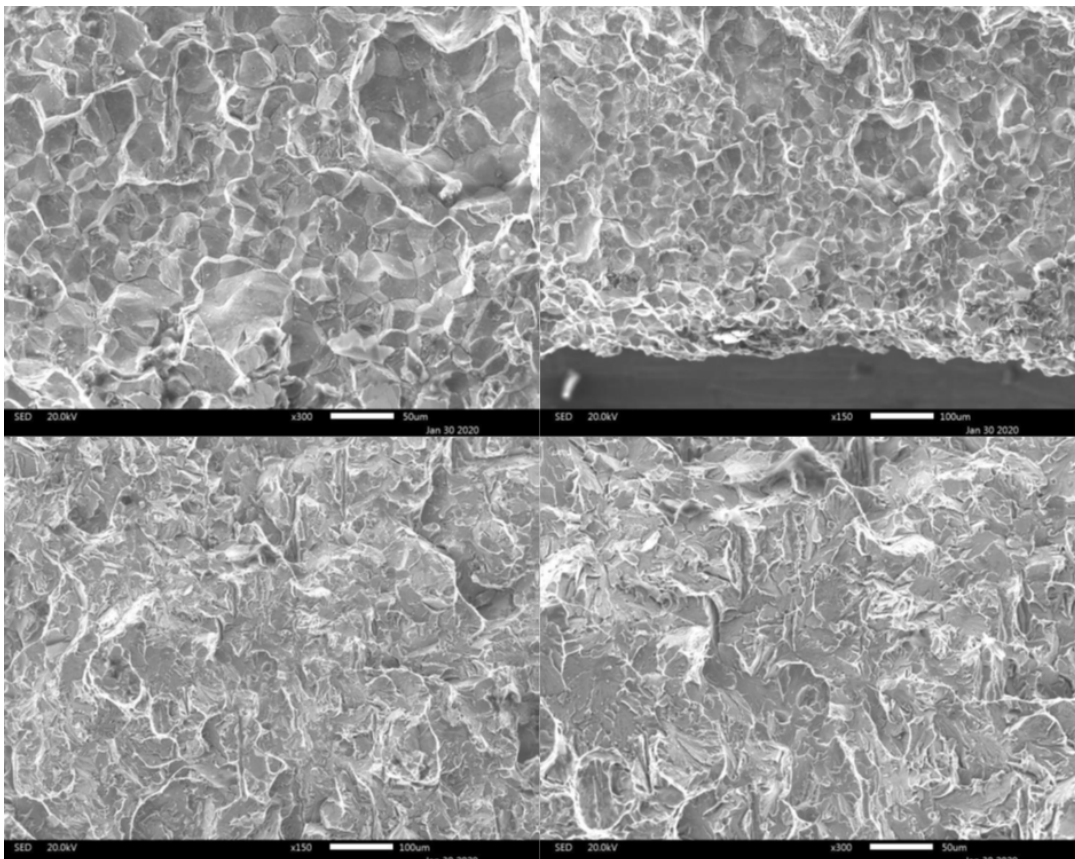


Figure 8. SEM images of different areas from the broken parts

ter structure and the determined core strength, it could be predicted that the component has little ductility and toughness. This can also be concluded with the presence of a shiny surface. However, in the area where the fracture occurred (FR sample), there is a mixed structure of bainite and coarse martensite phases also in the surface zone.

SEM images taken from the fracture surfaces with different magnifications are shown in Figure 8. It is seen from the figure that intergranular fracture (which is a sign of brittle fracture) is valid in the surface zone. And a mixed mode with cleavage type of fracture is visible in the core center part of the sample.

The polished cross section prepared from the radius area of the part is shown in Figure 9, and the hardness test results are given in Table 3 and Figure 10. It is known that Bainite phase is formed at slower cooling rates more than that for martensite formation and faster than that for ferrite and pearlite microstructure and martensite is formed when the cooling rate from austenitic microstructure is sufficiently fast. So, these hardness results confirm the microstructural analysis mostly.

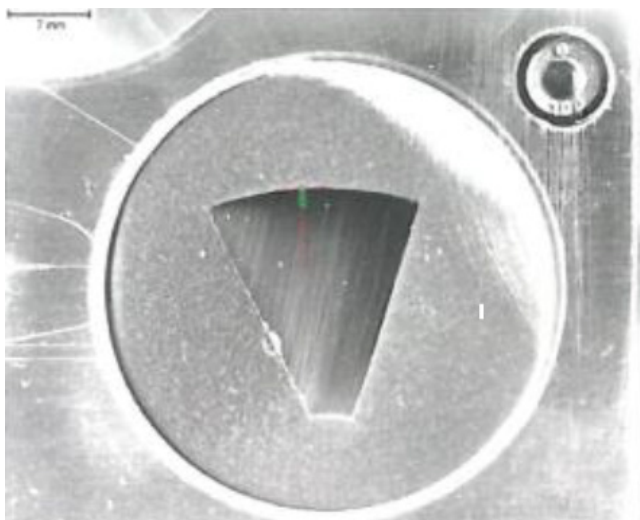


Figure 9. Prepared hardness test sample from the radius area

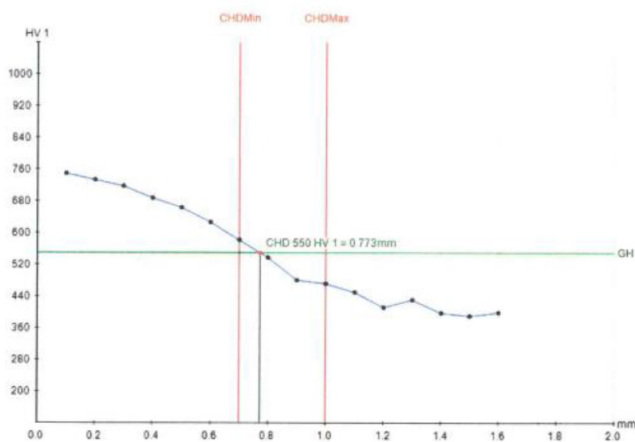


Figure 10. Graphical hardness test results of the RD sample

The polished cross section prepared from the fracture area of the part is shown in Figure 11, and the hardness test results are given in Table 4 and Figure 12.

Table 3. Hardness test results belong to RD sample.

Step	Result (HV)	X- Position (mm)	Y- Position (mm)	Hardness Depth 550 HV1
1	750	0,1	0	0,773 mm
2	734	0,2	0,2	
3	718	0,3	0	
4	688	0,4	0,2	
5	664	0,5	0	
6	627	0,6	0,2	
7	582	0,7	0	
8	538	0,8	0,2	
9	481	0,9	0	
10	472	1	0,2	
11	450	1,1	0	
12	412	1,2	0,2	
13	431	1,3	0	
14	398	1,4	0,2	
15	390	1,5	0	
16	399	1,6	0,2	

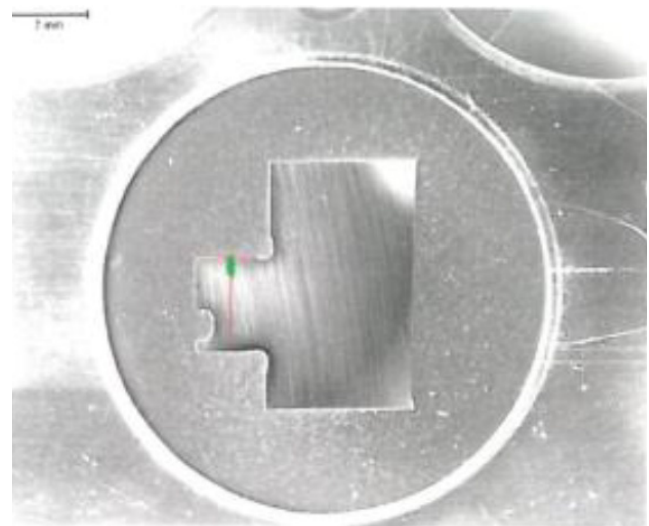


Figure 11. Prepared hardness test sample from the fracture area

Table 4. Hardness test results belong to FR sample.

Step	Result (HV)	X- Position (mm)	Y- Position (mm)	Hardness Depth 550 HV1
1	755	0,1	0	0,794 mm
2	751	0,2	0,2	
3	702	0,3	0	
4	680	0,4	0,2	
5	657	0,5	0	
6	613	0,6	0,2	
7	579	0,7	0	
8	548	0,8	0,2	
9	533	0,9	0	
10	509	1	0,2	
11	475	1,1	0	
12	461	1,2	0,2	
13	436	1,3	0	
14	435	1,4	0,2	
15	438	1,5	0	
16	425	1,6	0,2	

As a result of the analysis, the exact outcome reason of the fracture could not be determined as there are no clear signs of possible failure types such as hydrogen embrittlement

failure. The only clear outcome is the presence of the brittle type of fracture mode especially in the surface part, which is concluded by the help of the SEM study. With the present structure it is to be expected that even a low dynamic load can lead to the sudden failure. Hydrogen absorption with martensitic structure causes cracks to occur on the weakest point of part, especially on the steel parts which become particularly brittle.

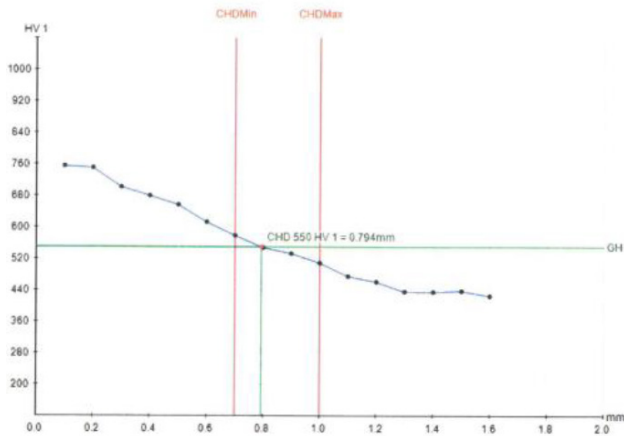


Figure 12. Graphical hardness test results of the FR sample

#### 4. CONCLUSIONS

This study was conducted on the parts those are used as pins in the truck axles, and this detailed examination has emerged due to the sudden break of the part during assembly. The fracture is a brittle one. Based on the core structure and the determined core strength, it can be assumed that the component has no very low ductility or toughness. With the present structure it is to be expected that even a low dynamic load can lead to breakage. As a result, the following conclusions can be drawn:

1. The metallographic examination shows that there is a martensitic hardness structure without mesh or bone carbide at the edge.
2. In the core there is an inhomogeneous mixed structure of bainite and coarse martensite components.
3. It can be assumed that the structure shows high strength.
4. The investigations carried out suggest that the component was exposed to incorrect heat treatment parameters.
5. As a result of the work, it has been concluded that the heat treatment of the parts is not homogeneously distributed and therefore fractures occurred.

It is a target to prevent premature failures that may occur due to material selection, design, manufacturing, or heat treatment. It is very important for heat treatment companies to understand the cause of the break and to work on this issue. In addition, engineers and designers need to understand the effect of heat treatment to eliminate problems related to longevity and service performance.

#### CONFLICT OF INTEREST

There is no conflict of interest in this article.

#### REFERENCES

- [1] Jaroslav, M. (2003). Finite element analysis and simulation of quenching and other heat treatment processes. *Computational Materials Science*, 27, 313-332.
- [2] Ono, T., & Allaire, R. A. (2000). Fracture analysis, a basic tool to solve breakage issues. Taiwan FPD Expo 2000.
- [3] Garcia, C., Martin, F., De Tiedra, P., Heredero, J. A., & Aparicio, M. L. (2001). Effects of prior cold work and sensitization heat treatment on chloride stress corrosion cracking in type 304 stainless steels. *Corrosion science*, 43(8), 1519-1539.
- [4] Goldstein, J. I., Newbury, D. E., Michael, J. R., Ritchie, N. W., Scott, J. H. J., & Joy, D. C. (2017). *Scanning electron microscopy and X-ray microanalysis*. Springer.
- [5] Budinski, K. G. (1988). *Surface Engineering for Wear Resistance*. (Retrospective Coverage). Prentice-Hall, Inc, Englewood Cliffs, New Jersey 07632, United States
- [6] Krauss, G. (1990). *Steels: heat treatment and processing principles*. ASM International, 497.
- [7] Drozda, T., & Wick, C. (1985). *Tool and Manufacturing Engineers Handbook: Materials, Finishing and Coating (Vol. 3)*. Society of Manufacturing Engineers.
- [8] Grube, W. L., & Gay, J. G. (1978). High-rate carburizing in a glow-discharge methane plasma. *Metallurgical Transactions A*, 9(10), 1421-1429.
- [9] Akiniwa, Y., Stanzl-Tschegg, S., Mayer, H., Wakita, M., & Tanaka, K. (2008). Fatigue strength of spring steel under axial and torsional loading in the very high cycle regime. *International Journal of Fatigue*, 30(12), 2057-2063.
- [10] Meyers, M. A., & Chawla, K. K. (2008). *Mechanical behavior of materials*. Cambridge university press.
- [11] Shipley, R. J., Becker, W. T., & ASM, H. V. (2002). *Failure analysis and prevention*. ASM handbook, 11, 508.
- [12] ASTM E 350 (2000). *Standard Test Methods for Chemical Analysis of Carbon Steel, Low-Alloy Steel, Silicon Electrical Steel, Ingot Iron, and Wrought Iron*, 2000.
- [13] SAE J 404 Standard, *Chemical Compositions of SAE Alloy Steels* (2009). *International Journal of Engineering Research & Science (IJOER)*, 2(6) June-, p. 109
- [14] ASTM E 112 (2006) *Standard Test Methods for Determining Average Grain Size*
- [15] ASTM A 370 (2007). *Standard Test Methods and Definitions for Mechanical Testing of Steel Products*.
- [16] Hull, D. (1999). *Fractography: observing, measuring and interpreting fracture surface topography*. Cambridge University Press.
- [17] Vargas-Arista, B., Teran-Guillen, J., Solis, J., García-Cerecero, G., & Martínez-Madrid, M. (2013). Normalizing effect on fatigue crack propagation at the heat-affected zone of AISI 4140 steel shielded metal arc weldings. *Materials Research*, 16(4), 722-778.
- [18] Shoffner, B. W. (2008). Development and validation of a finite element analysis model used to analyze coupling reactions between a tractor's fifthwheel and a semitrailer's kingpin.
- [19] Dieter, G. E., & Bacon, D. J. (1976). *Mechanical metallurgy (Vol. 3)*. New York: McGraw-hill.

- [20] Gao, F. M., & Gao, L. H. (2010). Microscopic models of hardness. *Journal of superhard materials*, 32(3), 148-166.